Nuclear Inst. and Methods in Physics Research, A 1046 (2023) 167661

Contents lists available at ScienceDirect

Nuclear Inst. and Methods in Physics Research, A

journal homepage: www.elsevier.com/locate/nima

# A SiPM-based optical readout system for the EIC dual-radiator RICH

Roberto Preghenella [a,*], Maxim Alexeev [e,f], Pietro Antonioli [a], Casimiro Baldanza [a], Luca Barion [c], Michela Chiosso [e,f], Marco Contalbrigo [c], Fabio Cossio [e], Silvia Dalla Torre [g], Manuel Dioniso Da Rocha Rolo [e], Giulio Dellacasa [e], Davide Falchieri [a], Roberto Malaguti [c], Marco Mignone [e], Luigi Pio Rignanese [a,b], Nicola Rubini [a,b], Simone Vallarino [c,d]

[a] *Istituto Nazionale di Fisica Nucleare, Sezione di Bologna, Italy*
[b] *Università di Bologna, Italy*
[c] *Istituto Nazionale di Fisica Nucleare, Sezione di Ferrara, Italy*
[d] *Università di Ferrara, Italy*
[e] *Istituto Nazionale di Fisica Nucleare, Sezione di Torino, Italy*
[f] *Università di Torino, Italy*
[g] *Istituto Nazionale di Fisica Nucleare, Sezione di Trieste, Italy*

ARTICLE INFO

*Keywords:*
EIC
RICH
SiPM

ABSTRACT

Silicon photomultipliers (SiPM) are candidates selected as the potential photodetector technology for the dual-radiator Ring-Imaging Cherenkov (dRICH) detector at the future Electron-Ion Collider (EIC). SiPM are cheap devices, highly efficient and insensitive to the high magnetic field at the expected location of the sensors in the experiment. On the other hand, SiPM are not radiation tolerant. Despite the integrated radiation level is expected to be moderate it should be tested whether single photon-counting capabilities and the increase in dark count rate can be kept under control to maintain the optimal dRICH detector performance across the years. The current status of the research for the EIC dRICH application and the first results on studies performed on a sample of commercial and prototype SiPM sensors are presented.

## 1. Introduction

The future Electron-Ion Collider (EIC) [1] is under development by a large international community and will be constructed in the USA in this decade and foreseen to start operation in the early 2030. One of the major challenges for the detectors at the EIC is particle identification (PID) [2]. A dual-radiator Ring Imaging Cherenkov (dRICH) detector [3] is identified as a compact and cost-effective solution for the broad momentum coverage required at forward rapidity: $3\sigma$ K/$\pi$ separation from a few GeV/c up to 50 GeV/c. The detector would consist of aerogel and gaseous ($C_2F_6$) Cherenkov radiators with refractive indices of ~ 1.02 and 1.0008, respectively. A readout surface of ~ 3 m$^2$ equipped with 3 × 3 mm$^2$ photosensor pixels (~ 300 k channels) must provide efficient single-photon detection inside a high magnetic field (~ 1 T). The photosensors are located outside of the detector acceptance, opening the possibility to explore the use of silicon photomultiplier sensors (SiPM) as an option for Cherenkov light readout [4]. The SiPM readout option has on one hand several advantages: SiPM are cheap sensors with high photodetection efficiency, excellent time resolution [5] and are insensitive to high magnetic fields. On the other hand they naturally present large dark count rates (DCR) and are prone to radiation damage [6], which increases currents and the DCR significantly.

The R&D being carried out aims at studying the radiation damage in SiPM and their usability for Cherenkov imaging application up to fluences of $10^{11}$/cm$^2$ 1-MeV neutron equivalent (simply $n_{eq}$ in the following), beyond the highest radiation level expected during dRICH operation. Several options are available to maintain the DCR to an acceptable rate (below ~ 100 kHz/mm$^2$), namely by reducing the SiPM operating temperature (cooling), using the timing information with high-precision TDC electronics (gating) and by recovering the radiation damage with high-temperature annealing cycles (curing). Encouraging results have been published on the performance of cooled SiPM after irradiation and annealing cycles [7]. Nonetheless, the limits on the usage of SiPM sensors depend on many factors and they should be tested for each specific application.

## 2. Irradiation and annealing

Custom carrier boards have been designed to host SiPM sensors arranged in a matrix of 3 × 3 mm$^2$ pixels (Fig. 1, left). This design was carefully chosen to allow the boards to withstand irradiation and high-temperature annealing cycles and have a form factor

* Corresponding author.
*E-mail address:* roberto.preghenella@bo.infn.it (R. Preghenella).

https://doi.org/10.1016/j.nima.2022.167661
Received 14 September 2022; Accepted 12 October 2022
Available online 23 October 2022
0168-9002/© 2022 Elsevier B.V. All rights reserved.

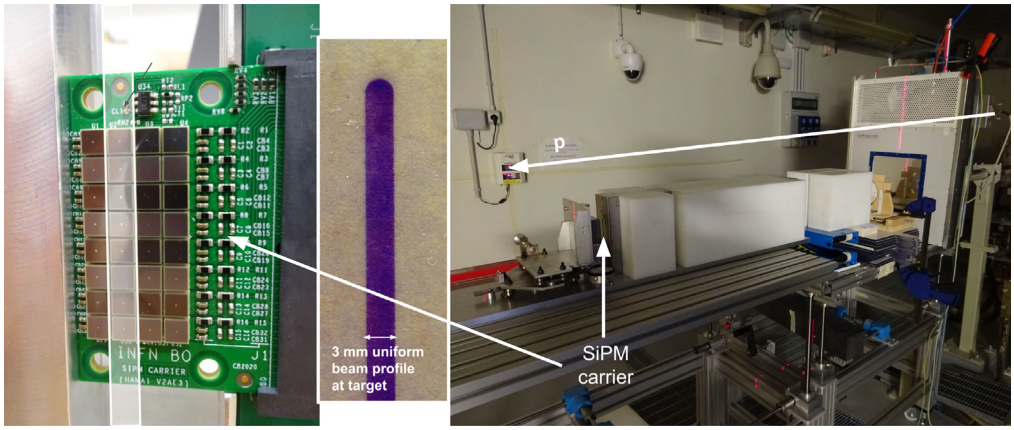


**Fig. 1.** (left) Custom SiPM carrier board. (centre) Uniform 3 mm irradiation field on a gafchromic film. (right) The collimator system on the irradiation beam line.

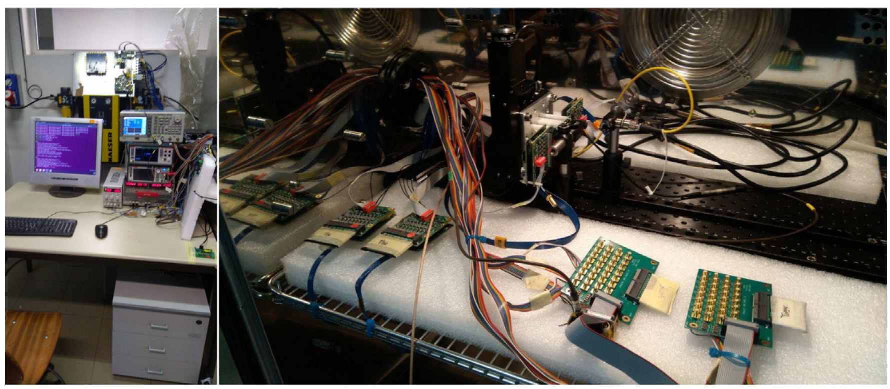

**Fig. 2.** Experimental equipment for SiPM characterisation outside (left) and inside (right) the climatic chamber.

usable for imaging in beam tests. The following boards and SiPM sensors have been irradiated: one board equipped with 16 Hamamatsu S13360-3050VS and 16 Hamamatsu S13360-3025VS sensors; one board equipped with 16 Hamamatsu S14160-3050HS and 16 Hamamatsu S14160-3015PS sensors; 2 boards each equipped with 12 NUV-HD-CHK and 12 NUV-HD-RH prototype sensors provided by Fondazione Bruno Kessler (FBK).

The SiPM sensors have been irradiated in the experimental room of the Trento Proton Therapy facility with 140 MeV protons produced in a large and uniform irradiation field [8]. The NIEL-scaling hypothesis is used to normalise the proton fluence to the corresponding 1-MeV neutron equivalent [9]. A dedicated collimator system (Fig. 1, right) has been designed to deliver the uniform irradiation field in a 3 mm wide window (Fig. 1, centre) such that thanks to a precision micrometric translation system a single column of sensors (8 SiPM) in the matrix is irradiated at a given time (Fig. 1, left)

For each board three different columns have been exposed at three different levels of irradiation: $10^9$, $10^{10}$ and $10^{11}$ $n_{eq}$. The fourth column was used to control the background neutrons generated by the scattering system and the collimators. Background neutrons received by each board are estimated to correspond to about 2–3 $10^8$ $n_{eq}$. The overall knowledge of the delivered neutron equivalent fluence is estimated to be of about 10%.

High-temperature annealing of the SiPM sensor boards has been performed with long (∼ 200 h) cycles up to 150 °C in a temperature-controlled climatic chamber ("oven" annealing).

## 3. Characterisation

Characterisation of the SiPM has been performed at $T = -30$ °C in a temperature-controlled climatic chamber on the sensors when new, after irradiation and after the high-temperature annealing cycles. Fig. 2 shows the characterisation setup with the experimental equipment located outside (left) and inside (right) the climatic chamber. Current measurements as a function of the bias voltage are performed in an automatised way by means of multiplexers that feed a Keithley 2450 source meter. DCR measurement as a function of the bias voltage are performed using a custom prototype electronics chain based on the ALCOR chip. ALCOR [10] is a prototype 32-pixel low-power mixed-signal ASIC developed to readout silicon photomultipliers at low temperature and performing single photon time-stamping. Configuration and readout of the ALCOR chip is performed via a Xilinx Kintex-7 FPGA KC705 evaluation board controlled by a Linux PC.

## 4. Results

Fig. 3 shows the dark current measured in FBK NUV-HD-CHK (left) and Hamamatsu S13360-3050VS (right) SiPM sensors. The dark current increases linearly with increasing fluence and decreases after high-temperature annealing. The amount of decrease measured in FBK sensors is of a factor ∼ 10 after annealing at $T = 125$ °C and of a factor ∼ 100 after annealing at $T = 150$ °C, corresponding to the dark current of sensors that have receive a factor 10 and 100 less fluence, respectively. A similar behaviour is observed in Hamamatsu sensors. Fig. 4 compares the measured DCR between different sensors at the same value of overvoltage before (left) and after (right) annealing. Hamamatsu S13360 sensors show the lowest DCR at all stages, starting from ∼ 1.5 kHz for new sensors up to ∼ 500 kHz for sensors irradiated with $10^9$ $n_{eq}$ before annealing and up to $10^{11}$ $n_{eq}$ after annealing.

The light response of irradiated and annealed Hamamatsu S13360 SiPM sensors coupled to the electronics has been studied with a pulsed-LED setup. Time coincidences between the recorded photon hit on the

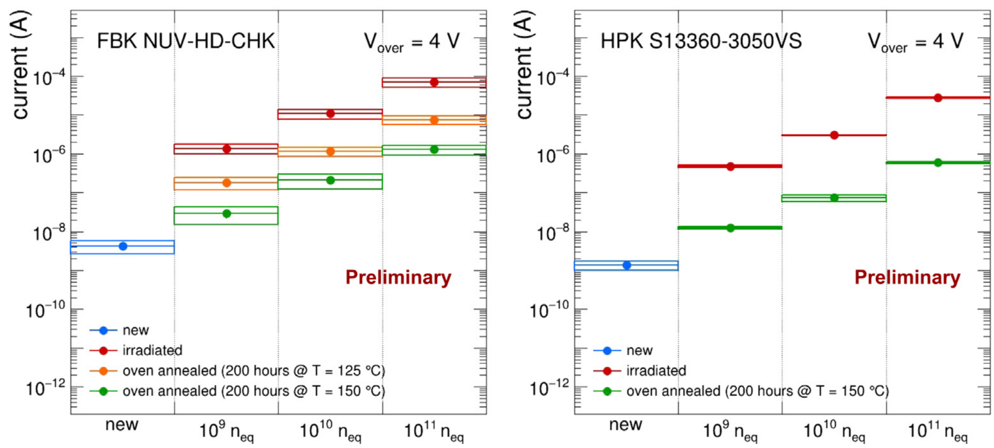


**Fig. 3.** Dark current measured in FBK (left) and Hamamatsu (right) sensors for different fluences and at different stages. The points represent the average over several sensors, whereas rectangles represent the RMS dispersion of the sample.

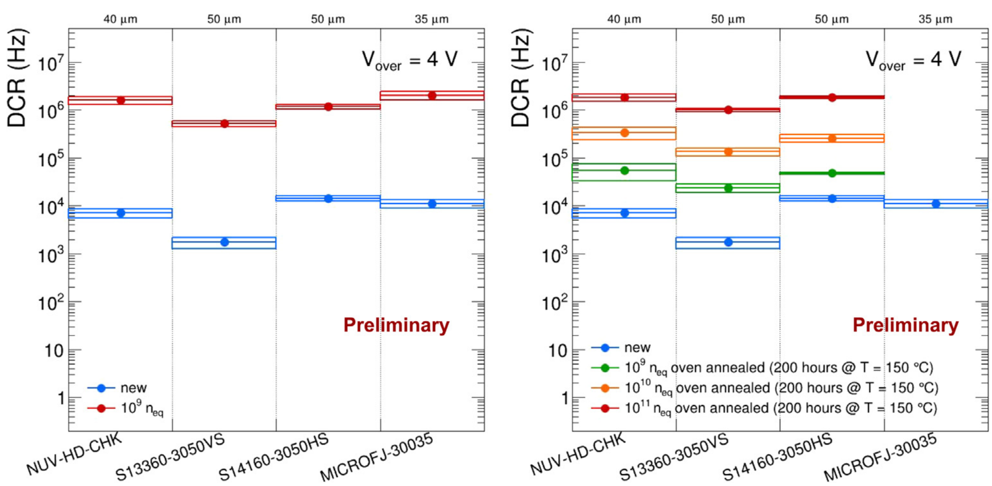


**Fig. 4.** Comparison of the measured DCR across different sensors before (left) and after (right) annealing. Also shown are measurements on SENSL MICROFJ-30035 sensors.

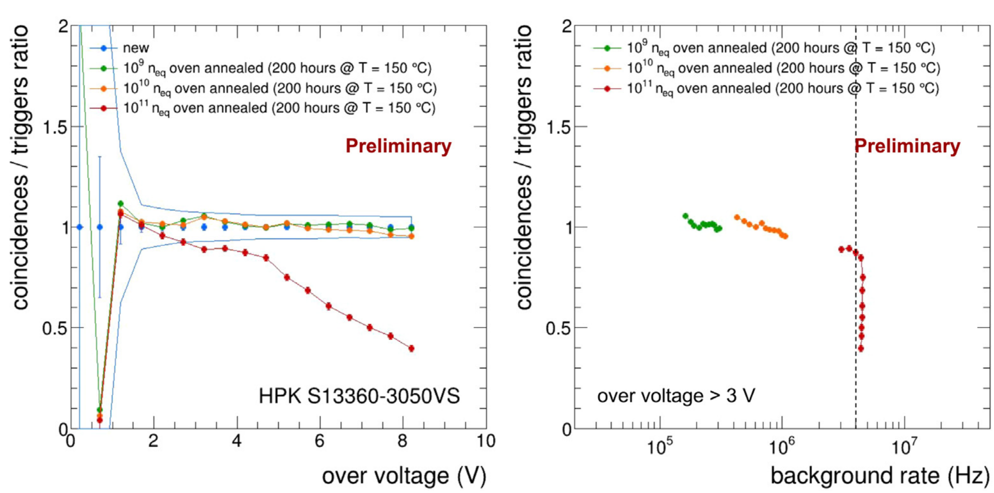


**Fig. 5.** Relative variation of PDE measured with pulsed LED light after irradiation and annealing as a function of bias voltage (left) and background rate (right).

sensor and the LED pulse are used to count the number of detected photons and as a proxy for the single-photon detection efficiency. While an absolute measurement of the PDE is not possible with this system, its relative variation can be measured with an estimated precision of 5%. Fig. 5 (left) shows the results of the relative variation of the PDE of irradiated and annealed sensors with respect to their performance measured when new. No loss in PDE is observed for sensors irradiated up to $10^{10}$ $n_{eq}$ and after high-temperature annealing. This proves that no damage on the sensors due to annealing procedure are observed within the accuracy of the measurement. An increasing PDE loss with increasing overvoltage is observed for sensors irradiated at $10^{11}$ $n_{eq}$ after high-temperature annealing, which is likely due to saturation

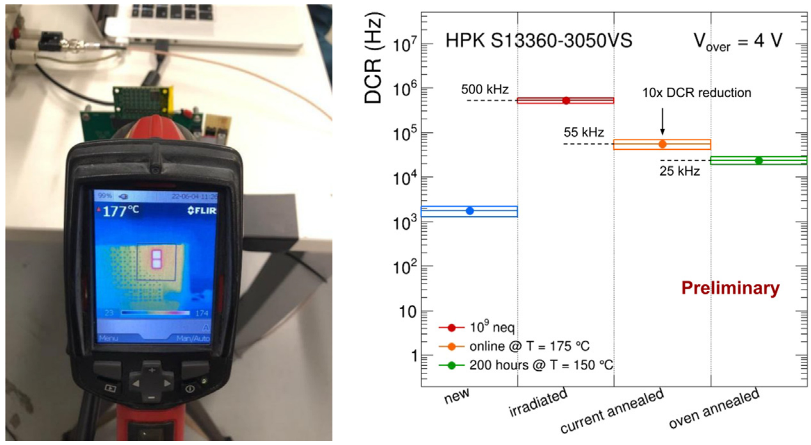


**Fig. 6.** (left) SiPM sensors undergoing the "online" annealing procedure are monitored with a thermal camera. (right) Comparison of the DCR measured after the "online" annealing procedure with other DCR measurements.

effects either in the readout electronics or signal overlaps over the large DCR background. Fig. 5 (right) shows that the loss in PDE starts when the background rate exceeds 4 MHz and hints at a saturation of counts in the ALCOR readout system.

An alternative procedure to the high-temperature annealing performed in the climatic chamber ("oven" annealing) was explored as a potential solution for annealing "in situ", that would allow curing the radiation damage without the need of removing the sensors from the dRICH in the experiment (online annealing). A few Hamamatsu S13360-3050VS sensors have been irradiated with 5 cycles of $2 \cdot 10^8$ $n_{eq}$ fluence each. Each irradiation cycle was interleaved by online annealing, forward biasing the sensor to deliver high current (corresponding to ∼ 1 W/sensor) for 30 min. A temperature of ∼ 175 °C was measured on the sensor surface by means of a thermal camera (Fig. 6, left) during the 30 min of the online annealing procedure. Preliminary results are shown in Fig. 6 (right) and are very encouraging. The sensors annealed with the "online" procedure show a factor 10 lower DCR than the irradiated sensors. While the "online" annealing procedure does not reach the recovery levels achieved with the "oven" annealing procedure, the method provides an effective and fast (100 times faster) cure of radiation damage that can be performed "in situ" and repeated as many times as needed. Further R&D will follow to consolidate the approach for EIC dRICH experimental case.

## 5. Conclusions

An R&D is ongoing to explore the use of SiPM as baseline for the EIC dRICH optical readout in conjunction with prototype chain of electronics based on the ALCOR front-end ASIC. Results on irradiation and high-temperature annealing over a large sample of devices show that the Hamamatsu S13360 sensors as the ones with the lowest DCR at all stages. Future studies foresee to perform repeated irradiation and annealing cycles to test the experimental scenario in a more realistic way. Preliminary studies based on forward-bias current annealing of the sensors show promising results, making the online annealing a valuable method for "in-situ" recovery and a "continuous" effective reduction of delivered fluence. Studies of single-photon light detection efficiency show that the SiPM performance is unaffected by irradiation and annealing up to $10^{10}$ $n_{eq}$, the observed efficiency loss at $10^{11}$ $n_{eq}$ is likely due to saturation of the electronics due to the very high background rate.

## Acknowledgements

This work is funded by the Commissione Scientifica Nazionale 3 (CSN3) of the Istituto Nazionale di Fisica Nucleare, Italy. This project has also received funding from the European Union's Horizon 2020 Research and Innovation programme under GA no 101004761 and GA no 824093. This work is supported by the U.S. Department of Energy, Office of Science, Office of Nuclear Physics under the EIC project number JSA-22-R412967. The authors would like to thank Francesco Tommasino and Enrico Verroi for the help with the irradiation at the Trento Proton Therapy facility.

## References

[1] A. Accardi, et al., Eur. Phys. J. A 52 (9) (2016) 268;
R. Abdul Khalek, et al., Nucl. Phys. A 1026 (2022) 122447.
[2] T. Ullrich, Nucl. Instrum. Meth. A 1039 (2022) 167041.
[3] A. Del Dotto, et al., Nucl. Instrum. Methods A 876 (2017) 237–240.
[4] I. Balossino, et al., Nucl. Instrum. Methods A 876 (2017) 89–92.
[5] S. Gundacker, et al., Phys. Med. Biol. 65 (2020) 025001.
[6] E. Garutti, Y. Musienko, Nucl. Instrum. Methods A 926 (2019) 69–84.
[7] M. Calvi, et al., Nucl. Instrum. Methods A 922 (2019) 243–249;
M. Cordelli, et al., JINST 16 (12) (2021) T12012.
[8] F. Tommasino, et al., Nucl. Instrum. Methods A 869 (2017) 15–20;
F. Tommasino, et al., Phys Med. 58 (2019) 99-106.
[9] A. Vasilescu, G. Lindstroem, http://rd50.web.cern.ch/NIEL.
[10] R. Kugathasan, JINST 15 (05) (2020) C05019.